New Phytologist

Research

Transcriptome profiles of hybrid poplar (*Populus trichocarpa* × *deltoides*) reveal rapid changes in undamaged, systemic sink leaves after simulated feeding by forest tent caterpillar (*Malacosoma disstria*)

Ryan N. Philippe[1,2], Steven G. Ralph[1,3], Shawn D. Mansfield[4] and Jörg Bohlmann[1,2,5]

[1]Michael Smith Laboratories, University of British Columbia, Vancouver, BC V6T 1Z4, Canada; [2]Department of Botany, University of British Columbia, Vancouver, BC V6T 1Z4, Canada; [3]Department of Biology, University of North Dakota, Grand Forks, ND 58202-9019, USA; [4]Department of Wood Sciences, University of British Columbia, Vancouver, BC V6T 1Z4, Canada; [5]Department of Forest Sciences, University of British Columbia, Vancouver, BC V6T 1Z4, Canada

Author for correspondence:
Jörg Bohlmann
Tel: +1 604 8220282
Email: bohlmann@msl.ubc.ca

Received: *9 April 2010*
Accepted: *14 June 2010*

New Phytologist (2010) **188**: 787–802
doi: 10.1111/j.1469-8137.2010.03392.x

Key words: galactinol synthase, herbivore defense, microarray, plant–herbivore interaction, poplar genome, source and sink relationships.

Summary

• Poplar has been established as a model tree system for genomic research of the response to biotic stresses. This study describes a series of induced transcriptome changes and the associated physiological characterization of local and systemic responses in hybrid poplar (*Populus trichocarpa* × *deltoides*) after simulated herbivory.

• Responses were measured in local source (LSo), systemic source (SSo), and systemic sink (SSi) leaves following application of forest tent caterpillar (*Malacosoma disstria*) oral secretions to mechanically wounded leaves.

• Transcriptome analyses identified spatially and temporally dynamic, distinct patterns of local and systemic gene expression in LSo, SSo and SSi leaves. Galactinol synthase was strongly and rapidly upregulated in SSi leaves. Genome analyses and full-length cDNA cloning established an inventory of poplar galactinol synthases. Induced changes of galactinol and raffinose oligosaccharides were detected by anion-exchange high-pressure liquid chromatography.

• The LSo leaves showed a rapid and strong transcriptome response compared with a weaker and slower response in adjacent SSo leaves. Surprisingly, the transcriptome response in distant, juvenile SSi leaves was faster and stronger than that observed in SSo leaves. Systemic transcriptome changes of SSi leaves have signatures of rapid change of metabolism and signaling, followed by later induction of defense genes.

Introduction

Poplar (*Populus* spp.) trees are ecological keystone species found throughout the northern hemisphere, often inhabiting riparian or plains environments (Whitham *et al.*, 1996). Throughout their lifetime (in some cases up to several hundred years), poplars are exposed to a large variety of insect pests, that inherently have the capacity to evolve at a much faster pace than the long-lived tree species. To cope with the unpredictable array of possible herbivores, poplars deploy a suite of constitutive and inducible, as well as direct and indirect defenses (Philippe & Bohlmann, 2007; Ralph, 2009). Induced defenses allow plants to allocate limiting resources for growth, development and reproduction when not under herbivore stress, which is of benefit for plant fitness (Baldwin, 1998; Mauricio, 1998; Strauss *et al.*, 2002). Poplars can induce defense responses systemically, that is throughout the plant (Parsons *et al.*, 1989; Arimura *et al.*, 2004; Babst *et al.*, 2009), thus providing undamaged tissues and organs with induced resistance to herbivory (Havill & Raffa, 1999).

Several recent studies have investigated the transcriptome responses in the damaged leaves of poplars challenged by real or simulated insect herbivory (Christopher *et al.*, 2004;

Lawrence *et al.*, 2006; Ralph *et al.*, 2006; Miranda *et al.*, 2007). Major & Constabel (2006) also compared damaged poplar leaves with undamaged systemic leaves of similar developmental stage (source leaves) and found extensive overlap in these gene expression profiles. Other work demonstrated the importance of source–sink relationships for induced defense in poplars and the heterogeneity of responses between the metabolically distinct leaf groups (Arnold & Schultz, 2002; Arnold *et al.*, 2004; Babst *et al.*, 2008). Recently, Babst *et al.* (2009) identified overlapping transcript profiles between systemic source and sink leaves of poplars in response to herbivory when a single time-point (22 h after treatment) of the defense response was analysed.

In order to identify spatial and temporal patterns of locally and systemically induced defense responses in sink and source leaves of hybrid poplar (*P. trichocarpa* × *deltoides*), we investigated transcriptome changes in leaves of different age and source/sink status over a time-course of 2–24 h after simulated insect attack. Oral secretions (OS) of forest tent caterpillars (FTC, *Malacosoma disstria*) induce gene expression in poplar and function as authentic mimics of insect herbivory when added to mechanical wounds (Major & Constabel, 2006). We report the analysis of transcriptome profiles of local (treated) source leaves (LSo), systemic (untreated) source (SSo) leaves, and systemic (untreated) sink (SSi) leaves in response to OS application. The results of this study highlight a rapid response in SSi leaves that is distinct compared to profiles from LSo and SSo leaves.

Materials and Methods

Plant and insect materials

All experiments were done with hybrid poplar (*P. trichocarpa* × *deltoides*, H11-11). Saplings were propagated, maintained in the glasshouse, treated, and harvested as described in Ralph *et al.* (2006). Source leaves (leaf plastochron index LPI 9+; Larson & Isebrands, 1971) and juvenile sink leaves (LPI 0–5) were collected for microarray analysis from trees of 150–200 cm in height (Fig. 1a,b). Rearing conditions for *M. disstria* Hübner (FTC) larvae were as described in Ralph *et al.* (2006). Collection of FTC OS is described in Philippe *et al.* (2009) (Fig. 1c). Unless otherwise stated, all reagents and solvents were from Fischer Scientific (Pittsburgh, PA, USA), Sigma-Aldrich (St. Louis,

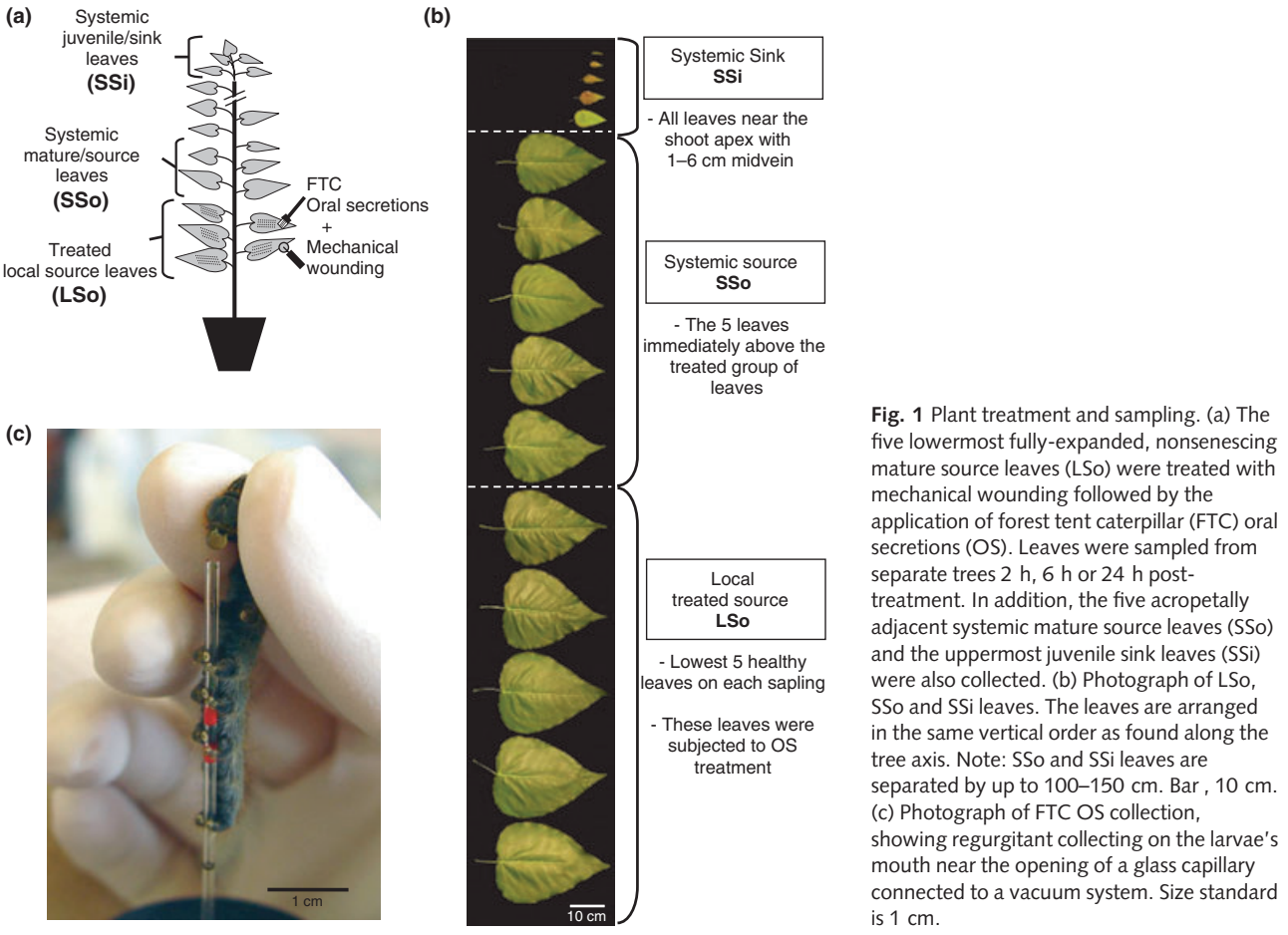

Fig. 1 Plant treatment and sampling. (a) The five lowermost fully-expanded, nonsenescing mature source leaves (LSo) were treated with mechanical wounding followed by the application of forest tent caterpillar (FTC) oral secretions (OS). Leaves were sampled from separate trees 2 h, 6 h or 24 h post-treatment. In addition, the five acropetally adjacent systemic mature source leaves (SSo) and the uppermost juvenile sink leaves (SSi) were also collected. (b) Photograph of LSo, SSo and SSi leaves. The leaves are arranged in the same vertical order as found along the tree axis. Note: SSo and SSi leaves are separated by up to 100–150 cm. Bar , 10 cm. (c) Photograph of FTC OS collection, showing regurgitant collecting on the larvae's mouth near the opening of a glass capillary connected to a vacuum system. Size standard is 1 cm.

MO, USA), EM Science (Darmstadt, Germany) or Invitrogen (Carlsbad, CA, USA).

Invertase assay

Sucrose cleavage by acid invertases was assayed by measuring the generation of glucose monomers following a protocol adapted from Arnold & Schultz (2002). Two-hundred milligrams FW of leaf material were ground in liquid nitrogen and extracted in 1 ml of buffer (150 mM Tris-HCl (pH 7.5), 2 mM EDTA, 10 mM ascorbic acid, 5% (w : v) polyvinylpolypyrrolidone (PVPP), 10 mM dithiothreitol (DTT), 2.5 mM benzamidine). Extracts containing soluble acid invertase activity were cleared by centrifugation for 15 min at 18 000 ***g***. Pellet containing cell wall bound acid invertase was washed three times and resuspended with 1 ml extraction buffer without PVPP. A volume of 600 μl of 100 mM sodium acetate (pH 4.5) and 200 μl of 100 mM sucrose were added to 200 μl of each of the two fractions, and incubated for 30 min at 37°C. Reducing sugars formed in the assay were detected with 3,5-dinitrosalicylic acid (DNS) according to Miller (1959), modified with the addition of 15-min incubation at 100°C before cooling to room temperature. Absorbance was measured at 560 nm. Acid invertase activities are reported as μmol sucrose cleaved per gram of tissue FW and minute.

Microarray and quantitative real-time PCR (qPCR) analyses

As described in Philippe *et al.* (2009), OS treatments consisted of leaves with four tracks of 10 cm-long wounds running parallel to the midvein, made with a fabric wheel, onto which 20 μl of OS was spread with a paintbrush (Fig. 1a). For each tree, the five lowest, fully-expanded, healthy leaves were treated. From each OS-treated and untreated control tree (no wound and no OS treatment) the five lowest healthy leaves (local source leaves; LSo), the five immediately adjacent fully expanded systemic leaves (systemic source leaves; SSo), and the five uppermost juvenile systemic leaves (systemic sink leaves; SSi) were collected at 2, 6 or 24 h after treatment (Fig. 1b), petioles removed, flash frozen in liquid nitrogen, and stored at −80°C. Total RNA was isolated, quantified, and checked for integrity and purity as described in Kolosova *et al.* (2004). Microarray experiments were designed to comply with MIAME guidelines (Brazma *et al.*, 2001). Details of the 15.5K poplar cDNA microarray platform (NCBI GEO platform number GPL5921) were described in Ralph *et al.* (2006). Microarray hybridizations, image capture and processing, data normalization and analysis were as previously described (Ralph *et al.*, 2006; Philippe *et al.*, 2009). Scanned microarray TIF images, the gene identification file, and ImaGene quantified data files are available at the NCBI GEO database http://www.ncbi.nlm.nih.gov/geo/query/acc.cgi?acc=GSE16383 (series GSE16383). Total RNA from source and sink leaves of OS-treated and untreated control trees was compared using a total of 54 hybridizations (see the Supporting Information, Fig. S1). Details of hybridization design and data analysis are described in Methods S1. The complete set of microarray results is available in Table S1. The qRT-PCR was done as previously described in detail in Ralph *et al.* (2006), with details of experimental design and analysis described in Methods S1; primers are listed in Table S2.

FLcDNA isolation of galactinol synthase (GOLS) genes

A TBLASTN search of the Treenomix poplar EST and FLcDNA database (Ralph *et al.*, 2006, 2008) was performed using plant GOLS nucleotide sequences available from GenBank. The CAP3 sequence assembly (Huang & Madan, 1999) was used to group expressed sequence tags (ESTs) into a total of seven different singletons and contigs (40 bp overlap, 95% identity). The corresponding cDNA clones were identified in library glycerol stocks, insert sizes determined and sequenced to high accuracy (GenBank accession numbers EU305718 to EU305724).

Analysis of GOLS sequences and phylogeny

Using BLASTP analyses of the 41 377 protein-coding gene loci predicted from the poplar genome sequence assembly v2.0 (http://www.phytozome.net/poplar) we identified GOLS genes in the *P. trichocarpa* Nisqually-1 genome (Tuskan *et al.*, 2006). As query sequences, we used plant GOLS sequences available in NCBI GenBank and the protein sequences deduced from the seven GOLS cDNAs identified in the Treenomix poplar EST collection. Alignments of multiple amino acid sequences were made with CLUSTALW (http://www.ebi.ac.uk/Tools/clustalw2) and BOXSHADE (bioweb.pasteur.fr/seqanal/interfaces/boxshade.html), and manually adjusted before maximum likelihood analysis using PHYML, version 2.4.4 (Guindon & Gascuel, 2003) with the JTT (Jones *et al.*, 1992) amino acid substitution matrix. The proportion of invariant sites and the alpha shape parameter were estimated by PHYML. Trees were generated using BIONJ (Gascuel, 1997), a modified neighbour-joining algorithm. SEQBOOT of the PHYLIP v3.66 package (Felsenstein, 1993; evolution.genetics.washington.edu/phylip.html) was used to generate 100 bootstrap replicates, which were then analysed using PHYML and the previously estimated parameters. CONSENSE, also from PHYLIP, was used to create a consensus tree. TREEVIEW (Page, 1996) was used to visualize the resultant trees. Bootstrap values above 80% were added to the maximum likelihood tree generated from the original dataset.

Analysis of galactinol and raffinose

Leaves were freeze-dried for 48 h. For each sample 50 mg leaf material was ground with a mortar and pestle in liquid nitrogen, and extracted for 24 h at −20°C with 4 ml of methanol–chloroform–water (12 : 5 : 3). Extracts were centrifuged for 10 min at 5000 ***g*** and 4°C, and the supernatant was collected. The pellet was washed with 8 ml of methanol–chloroform–water (12 : 5 : 3), centrifuged for 10 min at 5000 ***g*** and 4°C. Combined supernatants were mixed with 5 ml distilled water and, after phase separation, 1 ml of the aqueous phase was removed and dried at 40°C, resuspended in 1 ml distilled, deionized water and filtered through a 4 mm nylon filter (0.45 μm). Soluble carbohydrates were separated and quantified by anion exchange high-pressure liquid chromatography (HPLC) on a DX-600 ion chromatography system equipped with an AS50 autosampler and an ED50 electrochemical detector with gold electrode (Dionex, Sunnyvale, CA, USA). Monomeric sugars were isocratically separated with a 10 μl injection volume on a Carbopac PA-1 (Dionex) anion-exchange column (4 × 250 mm) with distilled, deionized water at room temperature at a flow rate of 1 ml min^{-1}, with a post-column addition of 100 mM NaOH before detection. Oligomeric sugars were isocratically separated with a 10 μl injection volume on a Carbopac MA-1 (Dionex) anion-exchange column (4 × 250 mm) with 300 mM NaOH at 0.3 ml min^{-1}. Fucose was used as internal standard for quantitative analysis. Sugar concentrations were determined using regression equations from calibration curves derived from standard solutions of galactinol and raffinose.

Results

Characterization of source–sink relationships

For the characterization of local and systemic responses to simulated insect feeding, we used the lowermost healthy LSo leaves, the immediately adjacent fully expanded SSo leaves and the uppermost juvenile SSi leaves (Fig. 1). As phloem connectivity influences spatial patterns of the systemic defense response in poplar (Davis *et al.*, 1991), we collected groups of five leaves for each leaf type to ensure that orthostichous phloem connections existed between the source and sink leaves (Larson, 1979). We measured soluble invertase (SI, Fig. 2a) and cell wall invertase (CWI, Fig. 2b) activity in leaves of untreated plants to determine the source–sink relationship between leaf groups that correspond to the LSo, SSo and SSi leaves in treated plants. The SI activity did not differ significantly between source and sink leaves (Tukey HSD: LSo vs SSo, $P = 0.998$; LSo vs SSi, $P = 0.998$; SSo vs SSi, $P = 0.999$); the OS treatment did not effect any significant change (Tukey HSD: LSo vs SSo, $P = 0.972$; LSo vs SSi, $P = 0.986$; SSo vs SSi, $P = 0.982$) either. In untreated plants, CWI activity was approximately twofold higher in sink leaves than in source leaves (Tukey HSD: LSo vs SSo, $P = 0.999$; LSo vs SSi, $P = 0.035$; SSo vs SSi, $P = 0.047$). In plants treated with OS, CWI activity increased about twofold relative to undamaged plants after 2 h in LSo, SSo and SSi leaves (Tukey HSD: LSo vs SSo, $P = 0.992$; LSo vs SSi, $P < 0.001$; SSo vs SSi, $P < 0.001$), maintaining the source–sink relationship and potentially increasing phloem loading/unloading capacities with treatment. Two-way ANOVA indicated that CWI activity was influenced by leaf type ($P < 0.001$) and by OS treatment ($P < 0.001$), though the interaction term was not significant ($P = 0.140$).

Overall spatial and temporal patterns of leaf transcriptomes in response to OS treatment

We used the poplar 15.5K cDNA microarray (Ralph *et al.*, 2006) to examine transcriptome changes in LSo, SSo and

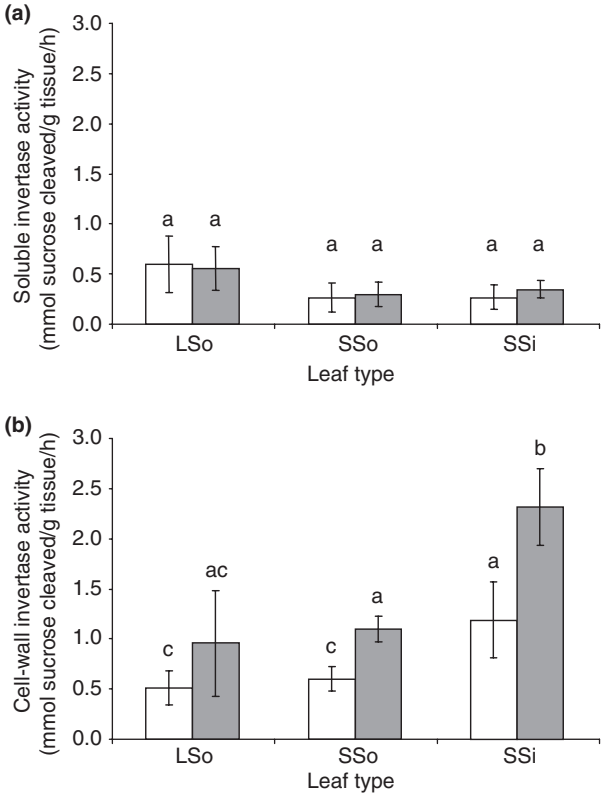

Fig. 2 Soluble (SI; a) and insoluble cell wall invertase (CWI; b) activity in source and sink leaves of untreated control and forest tent caterpillar (FTC) oral secretion (OS)-treated poplar trees 2 h after treatment. Open bars, SI or CWI activity in local source (LSo), systemic source (SSo) and systemic sink (SSi) leaves of untreated control trees; tinted bars, SI or CWI activity in LSo, SSo and SSi leaves of OS-treated trees. Values are mean ± SD ($n = 5$ trees). Data were analysed using two-factor ANOVAs and Tukey multiple comparison tests. Bars with different letters are significantly different at $P = 0.050$; letters are independent such that 'ac' is not significantly different from either 'a' or 'c', while 'a' and 'c' are significantly different from each other.

SSi leaves in response to OS treatment. Genes that showed changes in transcript abundance (i.e. differentially expressed (DE) genes) were identified using three criteria: at least a 1.5-fold change between the corresponding samples from treated trees and untreated control trees, a Student's *t*-test *P*-value < 0.05 and a *Q*-value < 0.05. Using these criteria, genes corresponding to approx. 40% of elements on the array were DE in treated trees. Approx. 20% were DE in only one leaf group, indicating leaf type-specific transcriptome responses. The complete set of expression data for all genes represented on the microarray is provided in Table S1.

To accommodate the large number of samples (90 trees for 18 different combinations of time points and leaf types; Fig. S1), the initial transcriptome profiling was done with pooled RNA from five biological replicates for each leaf type and time-point using a total of 54 array hybridizations. To validate these analyses and to assess the variability of the transcriptome responses, we performed additional hybridizations with RNA from each of four independent biological replicates comparing treatment and control of SSi leaves at the 2 h time-point. Results obtained from analysis of pooled and independent replicate samples showed similar variance (Fig. S2), confirming previous validations of microarray analyses with pooled samples from glasshouse-grown clonal poplar (Ralph *et al.*, 2006; Miranda *et al.*, 2007; Philippe *et al.*, 2009).

The overall spatial and temporal patterns of transcriptome changes in response to OS treatment revealed some substantial asymmetry in the three different leaf types (Fig. S3.) The response of LSo leaves to OS was strongest at 2 h (1568 genes upregulated, 938 downregulated) and 6 h (1624 genes upregulated, 900 downregulated) post-treatment with substantially fewer DE genes at 24 h (360 genes upregulated, 58 downregulated). In SSo leaves we detected a slower and weaker response induced by OS treatment with the largest number of upregulated transcript species observed at 24 h (411 genes upregulated, 74 downregulated). In contrast, of all three leaf types, SSi leaves showed the largest number of DE genes at the early time-point 2 h after treatment (1997 genes upregulated, 1632 downregulated). In summary, over the time-course of this analysis, LSo leaves responded rapidly and strongly, the observed response of SSo leaves was slower and weaker, and SSi leaves showed the fastest and strongest induced response.

qPCR reveals differential response of selected genes in source and sink leaves

To validate microarray analyses, we designed gene-specific primers (Table S2) for 10 DE genes and quantified their transcript abundance using qPCR (Fig. 3; Table S3). Genes were selected to cover a relevant range of treatment-induced DE from threefold (histone deacetylase; WS0158_D14; matches *Populus* v2.0 genome model POPTR_0009s15160; http://www.phytozome.net/poplar.php) to 24-fold (unknown protein; WS0123_C21; no match in *Populus* v2.0) change in transcript abundance according to microarray analysis. Expression patterns detected by microarrays were confirmed by qPCR for eight of the ten genes. The remaining two genes were from multigene families, and therefore transcript abundance measured with microarrays may be ambiguous. In general, we observed greater changes in transcript abundance by qPCR than by microarray hybridization. Significant OS-induced changes of transcript abundance ranged from 50-fold downregulation in SSi leaves at 24 h for a putative leucine-rich repeat (LRR) transmembrane protein kinase (WS0205_I02; POPTR_0002s14800) to 2235-fold upregulation for polyphenol oxidase (PPO; POPTR_0001s39660) in SSi leaves at 24 h.

The qPCR analysis confirmed that transcriptome changes differ between the three leaf types. For example, the gene with the strongest downregulated transcript abundance in SSi leaves at 2 h (15-fold down; LRR transmembrane protein kinase WS0205_I02; POPTR_0002s14800) showed a 1300-fold upregulation in SSo leaves, highlighting the differences in transcript response of the same gene between systemic source and sink leaves (Fig. 3). Other transcripts also showed upregulation in source leaves and downregulation in sink leaves (e.g. histone deacetylase WS0158_D14; POPTR_0009s15160) or vice versa (e.g. 9-*cis*-epoxycarotenoid dioxygenase WS0147_P16; POPTR_0019s12320). Some transcripts were most strongly upregulated in sink leaves (e.g. universal stress protein WS0124_D16; POPTR_0014s11710), while others responded most strongly in source leaves (e.g. aminopeptidase M, WS0212_I21; POPTR_0006s24090). We also found genes with upregulation across all three leaf types, with an observed maximum at 24 h (e.g. serine carboxypeptidase S28 WS0214_H20 (POPTR_0001s22060), endochitinase WS0143_A03 (POPTR_0009s14420), Kunitz protease inhibitor (KPI) WS0134_G14 (POPTR_0010s01150), polyphenol oxidase PPO (POPTR_0001s39660), and (−)-germacrene-D synthase TPS1 (POPTR_0001s44080)).

Cluster analysis reveals large-scale differences of OS-induced transcriptome responses in source vs sink and local vs systemic leaves

Next we comprehensively assessed the complete transcriptome data for possible differences in the response across the three different leaf types. Despite the large number of genes showing OS-induced changes in transcript abundance, there was relatively little overlap in the change of specific transcript species across all leaf types and time-points (Table S1), indicating that distinct sets of genes are affected by OS in different leaf types and that these gene sets are activated with temporally distinct profiles. We used the divisive DIANA algorithm (Bryan, 2004) for cluster analysis,

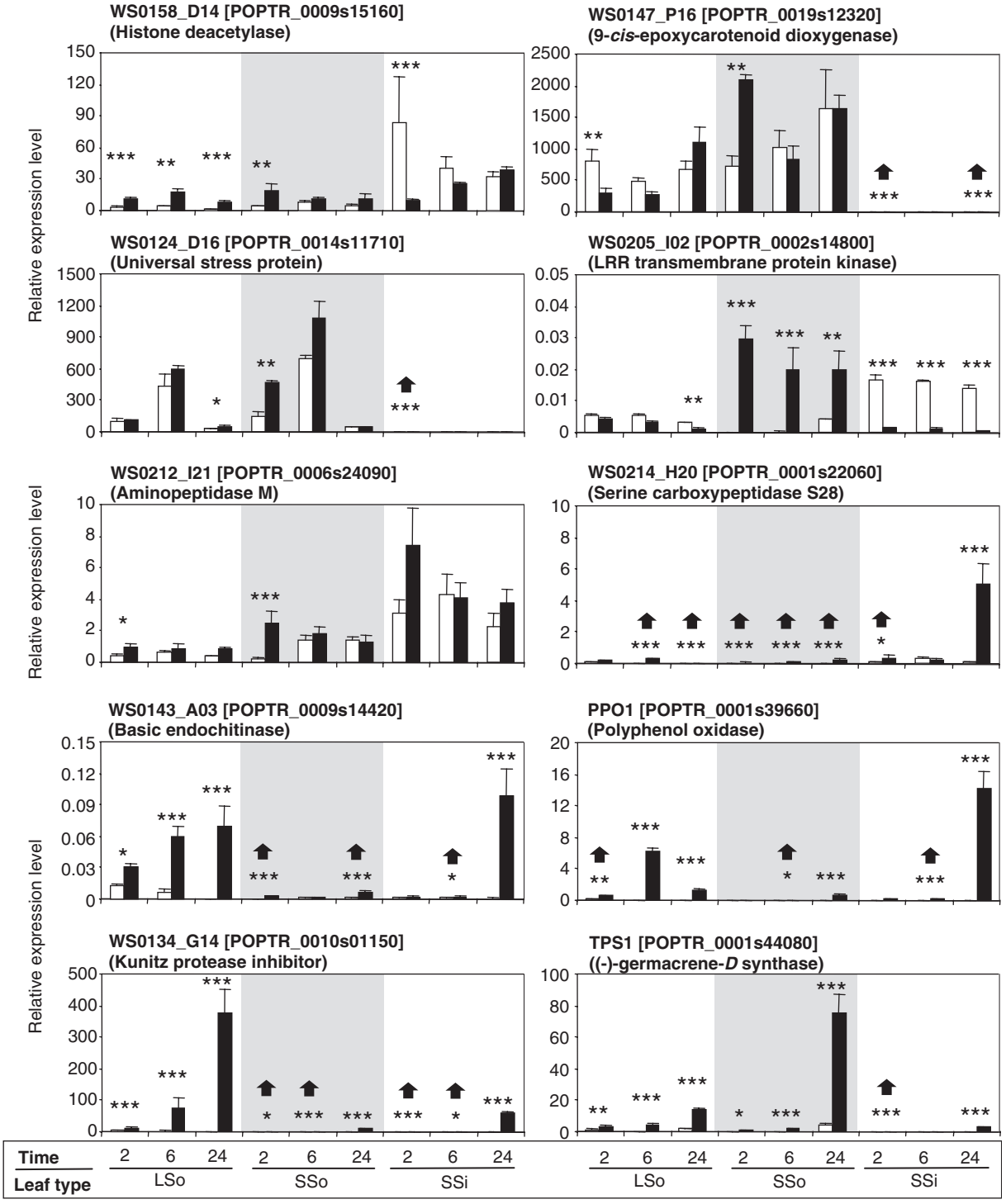

Fig. 3 Quantitative real-time PCR analysis of local and systemic gene expression of selected genes in poplar leaves in response to simulated forest tent caterpillar (FTC) herbivory. Transcript abundance for each gene was examined in local source (LSo), systemic source (SSo) and systemic sink (SSi) leaves at 2 h, 6 h and 24 h post-treatment. Transcript abundance was normalized to poplar translation initiation factor 5A (TIF5A; WS0116_J23; POPTR_0006s19870) by subtracting the Ct value of each transcript, where $\Delta Ct = Ct_{transcript} - Ct_{TIF5A}$. Transcript abundance of genes in control (open bars) and oral secretion (OS)-treated (closed bars) samples were obtained from the equation $(1 + E)^{-\Delta Ct}$, where E is the PCR efficiency, as described by Ramakers *et al.* (2003). A transcript with a relative abundance of one is equivalent to the abundance of TIF5A in the same tissue. Error bars show standard error. Statistical significance of expression differences relative to untreated plants was determined using a linear model (see the Materials and Methods and Table S3). Significance thresholds were set at * $P < 0.05$; ** $P < 0.01$; *** $P < 0.001$. Black arrows mark statistical differences where bars are small.

to identify global patterns of co-expressed genes in response to OS treatment (Fig. 4; Table S4). Transcripts corresponding to 7231 microarray elements with a fold-change > 1.5, $P < 0.05$ and $Q < 0.05$ in at least one leaf type and time-point in response to OS treatment fell into eight unique clusters showing distinct patterns of expression.

Four large clusters (clusters 1–4) identified in this analysis contain a total of 6841 genes, or 95% of all DE genes (Fig. 4). Cluster 1 contains genes that were upregulated early (2–6 h) mainly in LSo leaves. By contrast, cluster 3 contains genes that were upregulated early (2 h) mainly in SSi leaves, and cluster 4 contains genes that were downregulated early (2 h) mainly in SSi leaves. These three clusters identified genes with predominantly leaf type-specific responses. Cluster 2 contains genes that showed early (2–6 h) upregulation in SSi leaves and downregulation in LSo leaves. Many of the genes upregulated in LSo leaves identified in cluster 1 (1631, or 23%) have annotations associated with signaling, general stress response, primary metabolism or unknown functions (Table S4). The large number of genes in clusters 2, 3 and 4 (5210, or 72%) revealed that changes in SSi leaves comprise the major portion of the total OS-induced transcriptome response observed. These three clusters contain mainly genes annotated as functioning in primary metabolism or general stress responses (Table S4).

Substantially fewer genes are represented in the four additional clusters, 5–8. Cluster 5 contains the small number of genes whose transcripts were upregulated across all three leaf types and most rapidly and transiently increased with their observed peak at 2 h in the treated LSo leaves. This cluster contains genes annotated in primary metabolism, transport, signaling, redox reactions, flavonoid metabolism and volatile organic compound synthesis (Table S4). Cluster 6 also contains genes that responded throughout the plant, and more quickly in LSo leaves than in SSo or SSi leaves, but with overall slower response than genes in Cluster 5. This cluster contains a relatively high number of genes with putative functions in calcium binding or calcium signaling (Table S4). Cluster 7 contains genes with late or sustained response whose upregulation was greatest at 24 h throughout the plant. Genes of this cluster are annotated with functions in defense against insect herbivores, such as polyphenolic oxidase, Kunitz protease inhibitors, endochitinases or octadecanoid signaling, along with several apyrases (Table S4). The very small cluster 8 contains genes that respond in all three leaf types, were rapidly upregulated and were back to basal levels by 24 h in both LSo and SSo leaves, while peaking later at 6 h in SSi leaves. Thus, this cluster highlights differences between source and sink, as opposed to treated and systemic leaves.

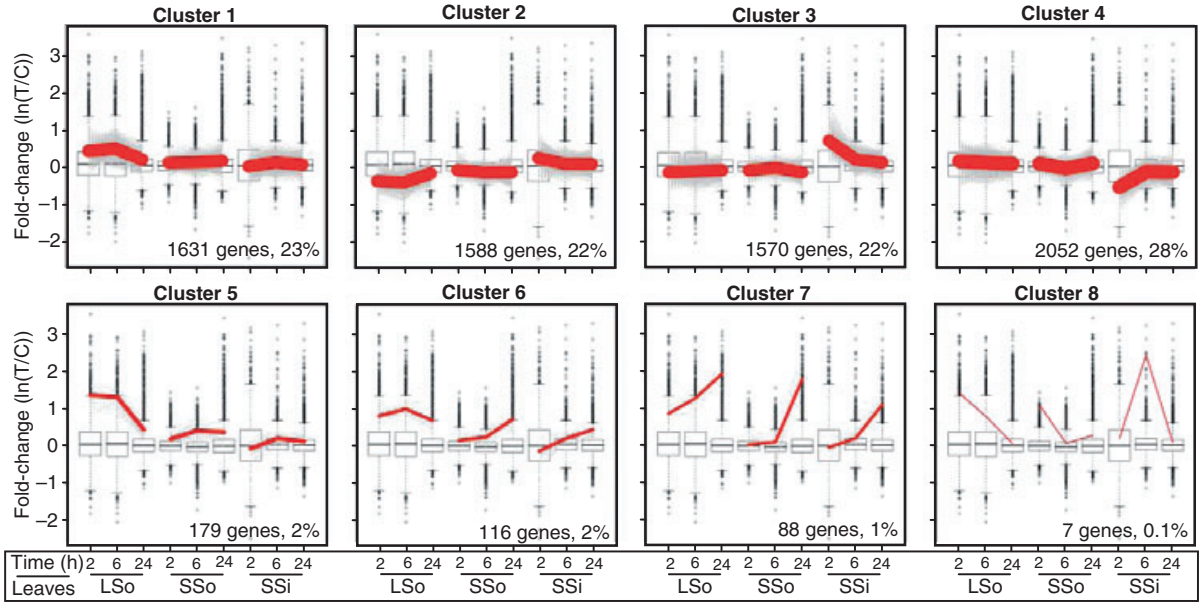

Fig. 4 Cluster analysis of expression profiles of differentially expressed (DE) genes. A set of 7231 genes were identified as DE (fold-change > 1.5 × for treated/control leaves; $P < 0.05$; $Q < 0.05$) for at least one time-point and leaf type and then clustered using the divisive DIANA algorithm (Bryan, 2004). For each panel, fold-change expression ratios are plotted for 2 h, 6 h and 24 h post-treatment for local source (LSo), systemic source (SSo) and systemic sink (SSi) leaves. Solid red lines represent the median expression ratio for a given cluster of gray lines, where each gray line represents the expression profile detected with an individual microarray element. For each leaf group, boxplot representations of the expression profile for the 7231 array elements included in this analysis are provided. Each boxplot shows the median value as a line dissecting the box, upper (75%) and lower (25%) quartiles at the top and bottom box edges, the nonoutlier minimum and maximum values as whiskers outside the box (1.5 × the interquartile range), and outlier values (beyond the whiskers) as open circles.

The cluster analysis supports the distinct spatial and temporal patterns of transcriptome changes noted in different leaf types with strong responses in LSo leaves, a strong early response in SSi leaves and the generally weaker and later response in SSo leaves.

SSi leaves show a unique and dynamic response to FTC OS

The contrast in expression profiles between LSo and SSi leaves shown by cluster analysis (Fig. 4) highlights the differences of temporal patterns of transcriptome changes between treated and systemic leaves, and between source and sink leaves. The strong early response in SSi leaves was particularly striking. For a more detailed investigation of the SSi leaf response, we identified the 20 most strongly upregulated and downregulated genes in these leaves at each time-point and compared their transcript abundance across LSo, SSo and SSi leaves (Tables 1, 2). For DE genes that are members of gene families where several members were among the most strongly responding genes, only a single representative is listed in Tables 1 and 2. For example, WS0133_I11 (POPTR_0010s01150) (Table 1) is shown to represent seven different KPIs that were found among the most strongly upregulated genes in SSi leaves at 24 h.

Genes with the strongest upregulation in SSi leaves at 2 h were not changed at the same time-point in SSo leaves, and many were substantially downregulated in LSo leaves at 2 h (Table 1, part a). Galactinol synthase was one of the most strongly upregulated at 2 h in SSi leaves (Table 1). A distinct fingerprint of strongly upregulated genes in SSi leaves was also seen at 6 h, although some of the same genes were also upregulated, albeit with lower fold-change, at 2 h in LSo and SSo leaves (Table 1, part b). The strongest upregulated transcripts in SSi leaves at 6 h grouped into a variety of heat-shock proteins and expressed protein of unknown function. At 24 h, the strongest-responding SSi genes were also highly upregulated in LSo and SSo leaves (Table 1, part c).

Results shown in Table 2 reveal that genes with the strongest downregulation in SSi leaves were practically unchanged in SSo leaves and possessed a relatively sparse and weak response in LSo leaves. Genes annotated as functioning mainly in transport and signalling are the most downregulated in SSi leaves at 2 h and 6 h, with heat-shock proteins appearing at 24 h. The strongest downregulated genes in SSi leaves at 2 h were not changed at the same time-point in SSo leaves, while the small proportion of responding genes in LSo leaves at 2 h (Table 2, part a) responded with weak upregulation and downregulation. An *O*-methyltransferase was one of the most strongly downregulated genes at 2 h in SSi leaves, with downregulation sustained at 6 h and lessening through 24 h (Table 2), mirrored by transient upregulation in LSo leaves at 2 h (Table 2, parts a and b). A distinct fingerprint of strongly downregulated genes in SSi leaves was also seen at 6 h, again with the near-absence of response in these genes in SSo leaves and weak response in a few genes in LSo (Table 2, part b). At 24 h, the strongest responding SSi genes were again mirrored by weak upregulation or downregulation in a few of the genes in LSo and SSo leaves (Table 2, part c). Interestingly, a quarter of the strongest downregulated genes in SSi leaves at 24 h were significantly downregulated earlier, at 2 h, with the majority of these being unknown genes.

The galactinol synthase (PtGOLS) gene family

Given the rapid and strong induction of transcripts for several GOLS genes in SSi leaves in response to OS-treatment, we characterized this gene family in poplar as a basis to explore the involvement of carbon metabolism in insect-induced defense responses. Nine unique gene predictions with sequence relatedness to functionally characterized plant GOLS were identified in the most recent assembly of the *P. trichocarpa* genome sequence. An additional gene model annotated as a putative galactinol synthase (POPTR_0010s24860.1) is more similar to glycosyl transferases when tested by BLAST against the NCBI nr database (data not shown), and was thus omitted from this analysis. The location of the *P. trichocarpa* (Pt)GOLS gene models on chromosome scaffolds is shown in Fig. 5. Based on amino acid sequence identity (Table S5), the nine predicted PtGOLS genes appear to have evolved from four ancestral genes through genome duplication. PtGOLS6g and PtGOLS7g are duplicated genes on chromosome scaffolds 2 and 14, respectively (93% amino acid sequence identity), as are the PtGOLS1g/PtGOLS8g and PtGOLS2g/PtGOLS9g pairs (89% shared identity within each pair) on chromosome scaffolds 8 and 10, although there has been an inversion in one of these last two PtGOLS gene pairs. PtGOLS5g is likely a duplicate of PtGOLS3g and PtGOLS4g (92% identity), where the last two genes appear to have arisen by tandem duplication within chromosome scaffold 13 (92% identity between PtGOLS3g and PtGOLS4g). These patterns of duplicated GOLS on different scaffolds are in agreement with the large-scale genome duplication and chromosome rearrangement patterns identified by Tuskan *et al.* (2006).

To verify the PtGOLS gene models predicted in the *P. trichocarpa* genome sequence (Fig. 5), we cloned seven different full-length (FL)cDNAs for GOLS genes (three from *P. trichocarpa*, four from *P. trichocarpa* × *deltoides*). The FLcDNAs nomenclature corresponds to the PtGOLS gene models based on sharing > 95% amino acid identity, with the .1/.2 designating putative alleles of the same gene (Fig. S4; Table S5). The predicted PtGOLSs share between 66% and 93% amino acid identity (PtGOLS2g and PtGOLS3g, and PtGOLS6g and PtGOLS7g, respectively) (Table S5). A carboxyl-terminal pentapeptide motif APSAA

Table 1 Top 20 microarray elements revealing strongest upregulated genes in systemic sink (SSi) leaves in response to mechanical wounding plus forest tent caterpillar (FTC, *Malacosoma disstria*) OS at 2 h, 6 h and 24 h. For comparison corresponding expression levels are also shown for treated local source (LSo) and systemic source (SSo) leaves[1]

	Clone ID	Match Genome[2]	Match AGI#	Annotation	*E*-value	LSo			SSo			SSi		
						2 h	6 h	24 h	2 h	6 h	24 h	2 h	6 h	24 h
(a)	**2 h**													
	WS0123_C21	n/a	n/a	No significant hit	n/a	1.16	0.93	0.95	1.10	1.01	0.91	24.63	1.72	1.37
	WS0124_D16	14s11710	At3g62550	Universal stress protein	9e-37	0.93	0.51	0.75	1.13	0.83	0.68	22.20	1.35	0.97
	WS01213_L10	08s19370	At1g60470	Galactinol synthase	3e-28	0.54	0.57	0.75	0.97	1.00	0.91	22.11	1.32	1.25
	WS0131_I20	14s03080	n/a	No significant hit	n/a	0.92	0.57	0.80	1.14	1.20	0.75	17.74	2.18	1.17
	WS0162_F09	15s06040	At4g23740	Leucine-rich repeat transmembrane protein kinase	2e-79	0.94	0.58	0.75	1.54	0.90	0.78	14.72	1.94	1.03
	WS01210_A07	39s00330	At5g53550	Oligopeptide transporter	2e-79	0.75	0.60	0.71	0.68	0.92	0.63	12.81	1.93	1.21
	WS0132_B08	17s06920	At2g24210	[Isoprene synthase] Terpene synthase TPS10	1e-8	0.58	1.06	0.77	0.81	0.94	0.75	11.79	1.31	1.03
	WS01213_O14	13s12390	At5g04530	KCS1 fatty acid elongase (3-ketoacyl-CoA synthase 1)	1e-38	0.82	1.08	1.34	0.87	0.75	0.58	11.29	1.53	1.15
	WS0152_B13	02s12840	n/a	No significant hit	n/a	0.37	0.40	0.89	0.85	0.74	0.79	10.90	1.81	0.97
	WS0162_D09	06s08780	At5g60020	Laccase / diphenol oxidase	3e-8	0.71	0.44	1.04	1.28	0.85	0.80	10.09	1.26	1.36
	WS0133_F02	02s08920	At1g24620	Polcalcin / calcium-binding pollen allergen	2e-22	0.62	0.44	0.75	0.79	0.81	0.69	9.84	1.49	1.04
	WS01117_C04	05s26930	At1g76180	Dehydrin (ERD14)	6e-10	0.70	0.50	0.80	1.01	0.78	0.76	8.59	1.02	1.06
	WS0134_L09	02s12850	n/a	No significant hit	n/a	0.46	0.60	0.60	1.14	0.78	0.65	8.31	2.08	1.05
	WS0178_N22	04s18200	At5g42190	E3 ubiquitin ligase SCF complex subunit SKP1/ASK1	1e-64	0.88	0.58	0.60	1.13	1.07	0.63	8.26	1.71	1.42
	WS0147_P16	19s12320	At4g19170	9-cis-epoxycarotenoid dioxygenase	1e-28	0.54	0.35	0.57	1.14	1.22	0.90	7.80	1.79	1.44
	WS0211_D07	16s14030	At5g05340	Peroxidase	3e-31	4.25	3.08	1.34	1.31	2.38	0.77	7.02	0.92	1.42
	WS0162_A24	16s08770	At2g37090	Glycosyl transferase family 43 protein	5e-68	1.05	0.79	0.99	0.84	1.02	1.01	7.00	1.64	1.64
	WS0143_H20	17s06670	At3g21890	Zinc finger (B-box type) family protein	5e-23	1.17	2.20	1.25	1.24	1.72	1.14	6.75	0.92	1.10
	WS0143_D11	13s06850	At2g30410	Tubulin folding cofactor A (KIESEL)	9e-18	0.85	0.56	0.87	0.91	1.21	0.84	6.67	1.24	1.18
	WS0162_F08	22s00830	At1g71900	Expressed protein	7e-15	1.01	1.37	0.72	0.90	1.21	0.80	6.03	1.16	2.11
(b)	**6 h**													
	WS0191_J03	09s15010	At2g29500	17.6 kDa class I small heat shock protein	2e-53	7.50	2.70	1.14	3.62	1.20	1.72	1.63	26.52	1.07
	WS02010_D03	04s07190	At5g52640	Heat shock protein 81-1	1e-31	3.74	2.04	1.01	2.80	0.99	0.95	1.14	12.81	1.20
	WS0202_P22	03s10860	At4g25200	23.6 kDa mitochondrial small heat shock protein	1e-51	4.45	2.47	1.07	3.19	0.98	1.46	0.93	12.40	1.49
	WS0231_D08	11s07550	At2g34070	Expressed protein	2e-43	1.75	1.31	1.06	1.63	1.02	0.94	2.49	12.30	1.08
	WS0172_K21	05s11910	At3g51130	Expressed protein	1e-84	5.89	2.42	1.21	2.93	0.88	1.28	1.44	10.49	0.85
	WS0192_G05	14s14690	At5g48570	Peptidyl-prolyl cis-trans isomerase	8e-21	3.11	2.04	1.14	3.07	1.03	1.63	0.76	8.19	1.17
	WS0178_C21	13s06780	At2g14880	SWIB complex BAF60b domain-containing protein	3e-23	2.40	1.85	0.90	2.09	1.16	1.15	1.16	8.08	1.01
	WS0162_E11	05s23040	At4g02830	Expressed protein	2e-14	1.56	2.25	1.02	1.21	1.12	1.50	0.74	6.93	0.68
	WS0211_C17	10s12370	At1g56300	DNAJ heat shock protein	1e-19	2.05	1.77	0.90	1.99	1.33	1.10	2.79	6.33	0.85
	WS0131_A16	256s00200	At1g17180	Glutathione S-transferase	1e-58	2.14	2.48	1.04	2.21	2.78	1.24	1.80	5.11	1.16
	WS01117_M09	03s18280	At1g16040	Phosphatidylinositol-glycan biosynthesis	3e-68	0.99	1.28	0.99	1.24	0.91	0.96	2.22	5.08	0.58
	WS0222_K18	09s16050	At2g27080	Harpin-induced protein-related	2e-60	1.71	1.37	1.09	2.53	2.65	1.41	1.97	4.93	1.21
	WS0208_H18	17s02810	At5g37670	15.7 kDa class I-related small heat shock protein	5e-44	1.70	1.43	1.19	2.21	0.91	1.21	0.53	4.49	1.04
	WS0132_I10	02s24310	At3g07090	Expressed protein	1e-32	2.14	1.86	0.89	1.83	1.99	1.67	1.28	3.90	1.19
	PX0015_F02	05s12410	At4g36600	LEA domain-containing protein	1e-10	1.68	1.27	1.01	2.58	2.82	0.92	1.11	3.72	1.57
	WS0195_F18	05s28110	At3g50770	Calmodulin-related protein	7e-17	2.85	1.63	1.12	1.22	1.41	1.53	2.56	3.49	0.87
	WS0204_K06	15s12060	At5g07330	Expressed protein	1e-29	1.15	1.04	0.82	1.32	0.83	1.13	1.34	3.48	0.92
	WS0132_E12	10s21350	At3g12580	Heat shock protein 70	3e-78	2.07	2.58	0.80	1.29	2.62	1.07	0.70	3.47	0.98
	WS0163_C23	07s01500	At2g30700	Expressed protein	6e-23	1.08	1.32	1.12	1.27	1.02	1.20	1.33	3.38	0.88
	WS0145_K16	08s22840	At5g18600	Glutaredoxin family protein	2e-38	1.41	1.45	1.03	1.30	1.25	1.26	0.72	3.36	0.71
(c)	**24 h**													
	WS0146_J02	04s18880	At3g12500	Basic endochitinase	6e-25	0.70	1.26	20.74	0.92	0.47	32.33	3.12	2.35	27.91
	WS0162_C15	08s12620	At2g01270	Thioredoxin	2e-41	1.39	5.80	3.21	1.19	1.93	3.86	0.80	1.64	13.40
	WS0212_O05	06s28990	At2g24520	ATPase, plasma-membrane-type	3e-97	2.06	2.47	11.21	0.79	0.84	6.88	2.32	1.34	10.71
	WS0212_I21	06s24090	At4g33090	Aminopeptidase M	3e-66	2.09	2.77	10.28	1.16	0.70	11.79	1.88	1.67	9.27
	WS0133_I11	10s01150	At1g17860	Kunitz protease inhibitor	3e-6	2.42	2.38	7.82	0.97	0.61	10.29	1.71	1.64	8.65
	PPO	01s39660	n/a	Polyphenolic oxidase	n/a	1.66	6.17	3.38	0.94	1.17	1.94	1.40	1.38	8.15
	WS0212_O01	07s11000	At4g36980	Expressed protein	2e-19	1.94	3.69	10.10	1.20	0.71	9.38	1.78	1.50	7.34
	TPS1	01s44080	n/a	(-)-germacrene-D synthase	n/a	1.94	9.64	3.04	1.10	3.26	2.68	3.08	1.20	6.86
	WS0214_H20	01s22060	At5g22860	Serine carboxypeptidase S28	1e-38	2.30	3.99	1.72	1.21	1.35	1.48	1.61	1.18	6.65
	WS0141_I19	06s11980	n/a	No significant hit	n/a	1.80	2.25	9.47	0.95	0.71	7.28	1.47	1.17	6.39
	WS0152_K23	08s00830	At4g29905	Expressed protein	3e-10	2.18	2.33	11.47	1.15	0.59	6.56	1.10	1.05	5.42
	WS01120_O24	02s11490	At4g07960	Glycosyl transferase family 2 protein	4e-13	1.88	2.39	5.95	1.19	0.76	7.19	1.08	1.04	5.00
	WS01120_K16	03s14550	n/a	No significant hit	n/a	3.42	7.52	12.11	1.19	2.13	18.77	0.88	1.76	4.79
	WS0141_A03	04s12470	At5g39410	Expressed protein	3e-42	2.51	2.42	11.93	1.05	0.75	3.65	1.31	1.47	4.60
	WS0212_C15	01s05560	At5g12950	Secreted protein SCF41.30c	2e-38	1.81	2.35	10.82	1.06	0.62	13.87	0.82	0.83	4.43
	WS0144_M15	10s16070	At3g17210	Stable protein 1	6e-36	2.09	2.76	3.67	1.16	1.33	3.73	0.79	1.30	3.83
	WS0156_A09	09s07810	At2g30080	Metal transporter ZIP6	9e-51	1.48	2.39	6.18	0.86	0.82	2.10	1.40	1.09	3.45
	WS01211_J20	06s28210	At5g10780	Expressed protein HSPC184	7e-13	1.35	1.97	8.37	0.80	0.84	2.74	0.91	0.95	3.44
	WS01118_E01	13s03860	At1g04240	Auxin-responsive protein	3e-35	2.84	3.60	9.52	1.17	0.71	3.03	1.00	1.81	3.42
	WS0178_N24	16s12600	At2g29420	Glutathione S-transferase	4e-27	3.27	4.76	7.60	1.32	1.91	11.66	0.79	1.95	3.24

[1]Microarray elements ranked by fold-change (FC) induction of response in SSi leaves to mechanical wounding plus FTC OS vs untreated control at 2 h, 6 h and 24 h, with FC values for those elements from LSo and SSo leaves also included for comparison. Subsequent redundant examples of a gene family at each time-point are removed to improve the diversity of different families included. Only FC values with statistical significance ($P < 0.05$, $Q < 0.05$) are coloured as different from '–' ('no change') according to the colour scale shown at right, where dark green to dark red correlates with the listed fold-change in expression. Abbreviations: AGI, *Arabidopsis* genome initiative; *E*-value, Expect-value; OS, oral secretions.

[2]Genome model names have the 'POPTR_00' prefix removed to fit the table.

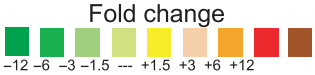

Table 2 Top 20 microarray elements revealing strongest downregulated genes in systemic sink (SSi) leaves in response to mechanical wounding plus forest tent caterpillar (FTC, *Malacosoma disstria*) OS at 2 h, 6 h and 24 h. For comparison corresponding expression levels are also shown for treated local source (LSo) and systemic source (SSo) leaves[1]

	Clone ID	Match Genome[2]	Match AGI#	Annotation	*E*-value	LSo			SSo			SSi		
						2 h	6 h	24 h	2 h	6 h	24 h	2 h	6 h	24 h
(a)	**2 h**													
	WS01214_O21	13s13990	At1g51990	O-methyltransferase family 2 protein	3e-43	1.781	1.208	1.103	1.209	1.166	1.392	0.085	0.503	0.711
	WS0161_F05	03s01440	At5g64080	Protease inhibitor/seed storage/lipid transfer protein	3e-12	0.783	1.553	1.484	1.231	0.985	0.896	0.104	0.419	0.495
	WS01217_E22	01s47550	n/a	No significant hit	n/a	2.030	1.426	0.781	1.280	1.041	1.063	0.154	0.723	1.398
	WS01224_K23	09s10800	At1g47480	Expressed protein similar to PrMC3 [Pinus radiata]	5e-23	1.069	1.353	0.690	1.229	1.115	1.239	0.172	0.600	0.763
	WS0162_B16	02s12780	At5g42890	Sterol carrier protein 2 (SCP-2) family	2e-46	0.696	1.893	2.273	1.340	1.067	1.602	0.191	0.915	2.377
	WS0119_H17	09s03410	At2g28790	Osmotin-like protein	6e-70	0.530	0.743	1.255	1.647	0.699	1.459	0.199	0.862	0.729
	WS01210_K09	06s10860	At2g38540	Nonspecific lipid transfer protein 1 (LTP1)	1e-30	0.672	1.586	2.255	1.519	0.997	1.281	0.222	0.843	0.372
	WS0111_L14	13s02990	At1g54690	Histone H2A	2e-48	1.265	1.138	1.132	1.292	0.985	1.220	0.222	0.984	0.758
	WS01121_O21	01s30920	At4g34160	Cyclin delta-3 (CYCD3	2e-65	0.961	0.789	0.851	1.619	0.903	0.857	0.226	0.964	1.237
	WS0122_I23	08s23110	n/a	No significant hit	n/a	1.520	1.255	1.074	1.047	1.016	1.246	0.227	0.541	0.606
	WS0175_M22	16s00270	n/a	No significant hit	n/a	1.145	0.946	1.080	1.334	1.140	1.166	0.236	0.610	0.615
	WS0224_G08	05s25620	At1g05150	Calcium-binding EF hand family	2e-65	0.711	0.772	0.983	0.569	0.892	0.770	0.242	0.666	0.849
	WS0221_M18	01s25490	At2g29570	Proliferating cell nuclear antigen 2 (PCNA2)	2e-60	0.733	1.019	0.862	1.487	1.019	1.228	0.252	0.728	0.784
	WS0113_K07	03s22240	At5g65360	Histone H3	3e-61	0.742	0.808	0.783	1.200	0.820	0.946	0.252	1.036	1.012
	WS02011_J14	06s11500	At3g54220	Scarecrow transcription factor	9e-63	0.919	0.477	0.702	1.083	0.891	1.127	0.253	0.836	1.158
	WS0116_O08	01s31790	n/a	No significant hit	n/a	1.009	0.986	1.221	1.667	0.926	1.752	0.255	0.868	0.969
	WS0195_A08	01s00240	At2g45190	Axial regulator (YABBY1)	1e-59	1.024	0.870	0.828	0.985	1.432	1.065	0.257	0.951	1.005
	WS02011_L19	07s08070	At5g60990	DEAD/DEAH box helicase	3e-30	1.473	1.061	0.874	1.034	0.892	0.826	0.259	0.908	0.878
	WS0166_C23	19s00770	At5g63660	Plant defensin-fusion protein, putative (PDF2.5)	4e-13	1.155	1.078	0.965	1.250	0.763	1.119	0.263	0.464	0.623
	WS0181_G13	12s11570	At5g61670	Expressed protein	7e-95	0.790	0.732	0.619	0.824	1.164	1.003	0.268	1.078	1.388
(b)	**6 h**													
	WS0158_J16	19s11560	At1g71880	Sucrose transporter (SUC1)	1e-06	0.404	0.536	0.605	0.797	0.691	0.919	1.354	0.324	1.398
	WS0185_D19	18s03570	At5g10695	Expressed protein	1e-23	0.312	0.340	1.130	1.122	0.433	0.883	1.208	0.391	0.613
	WS0161_F05	03s01440	At5g64080	Protease inhibitor/lipid transfer protein (LTP)	3e-12	0.783	1.553	1.484	1.231	0.985	0.896	0.104	0.419	0.495
	WS0125_C20	13s03890	At3g04720	Hevein-like protein (HEL)	7e-46	0.934	1.078	1.108	1.189	1.130	1.099	0.317	0.421	0.626
	WS01222_I21	01s39660	n/a	No significant hit	n/a	0.646	0.830	1.005	0.949	1.077	1.598	0.366	0.427	0.982
	WS0143_J07	01s03470	At1g80920	DNAJ heat shock protein	3e-33	0.384	0.425	1.005	0.735	0.368	0.742	0.805	0.442	0.455
	WS0166_C23	19s00770	At5g63660	Plant defensin-fusion protein, putative (PDF2.5)	4e-13	1.155	1.078	0.965	1.250	0.763	1.119	0.263	0.464	0.623
	WS0174_G20	05s23220	At1g03140	Splicing factor Prp18 family protein	7e-41	1.362	1.358	1.122	0.932	0.880	1.246	0.852	0.478	1.138
	WS01215_E16	03s10270	At1g31812	Acyl-CoA binding protein	1e-31	0.984	1.150	1.550	1.533	1.104	1.124	0.848	0.479	0.799
	WS0221_N18	07s10350	At2g23170	Auxin-responsive GH3 family protein	3e-72	1.141	0.752	0.947	1.044	1.229	1.306	0.421	0.485	0.773
	WS01218_M12	07s07110	n/a	No significant hit	n/a	0.672	0.720	0.894	1.121	0.682	0.777	0.694	0.500	0.880
	WS0113_N01	04s18240	At2g16850	Plasma membrane intrinsic protein, putative (SIMIP)	9e-64	0.687	0.920	1.091	1.501	1.394	1.756	0.647	0.501	0.435
	WS01214_O21	13s13990	At1g51990	O-methyltransferase family 2 protein	3e-43	1.781	1.208	1.103	1.209	1.166	1.392	0.085	0.503	0.711
	WS0199_D12	16s05020	At3g12150	Expressed protein	3e-60	0.726	0.880	0.989	1.051	0.973	1.181	0.751	0.505	0.869
	WS0113_J12	10s21590	n/a	No significant hit	n/a	0.924	1.239	1.306	1.344	1.004	0.955	0.773	0.509	0.908
	WS01127_I15	n/a	At3g10390	Amine oxidase family protein	5e-08	1.177	0.751	1.058	0.742	0.942	0.888	0.495	0.510	0.839
	WS01212_F14	06s01020	At3g22120	Protease inhibitor/lipid transfer protein (LTP)	2e-18	1.191	1.223	1.067	1.103	0.995	0.827	0.280	0.513	0.728
	WS01218_H13	10s19490	At3g55990	Expressed protein contains	7e-09	1.095	0.871	1.301	1.024	0.721	0.498	0.693	0.513	1.423
	WS0193_L20	15s08290	At5g14920	Gibberellin-regulated family protein	9e-23	0.795	1.096	0.850	0.751	0.754	0.694	0.345	0.516	0.779
	WS02012_E04	04s17490	n/a	No significant hit	n/a	1.053	1.239	1.073	1.014	1.127	0.970	0.505	0.518	0.939
(c)	**24 h**													
	WS0188_A14	05s02270	At5g27860	Expressed protein	1e-10	1.728	1.988	1.230	0.920	1.510	0.902	1.311	1.228	0.261
	WS0151_F02	04s17810	At2g17880	DNAJ heat shock protein	2e-27	0.243	0.192	0.872	0.720	0.290	0.440	0.826	0.683	0.343
	WS0151_H13	08s06260	At5g59720	18.1 kDa class I heat shock protein	2e-49	3.007	1.567	1.154	3.277	0.897	1.478	1.237	1.602	0.365
	WS01210_K09	06s10860	At2g38540	Nonspecific lipid transfer protein 1 (LTP1)	1e-30	0.672	1.586	2.255	1.519	0.997	1.281	0.222	0.843	0.372
	WS0224_E05	05s17200	At4g08950	Phosphate-responsive protein, putative	1e-87	1.523	1.639	1.256	0.610	0.901	1.201	1.003	0.815	0.388
	WS01217_C21	04s02340	n/a	No significant hit	n/a	1.442	0.973	1.978	1.201	1.145	1.234	0.563	0.815	0.397
	WS0141_D19	06s24030	At5g12020	17.6 kDa class II heat shock protein	1e-36	3.037	1.391	1.336	2.166	0.685	1.150	0.861	0.993	0.402
	PX0011_G05	10s20310	n/a	No significant hit	n/a	0.997	0.580	1.428	1.770	0.746	1.402	0.290	0.638	0.408
	WS0154_I03	15s06000	n/a	No significant hit	n/a	1.590	3.022	2.694	1.130	1.045	1.124	0.433	0.647	0.419
	WS0121_D17	08s06940	n/a	No significant hit	n/a	1.499	1.594	1.429	0.774	1.390	0.957	0.813	1.250	0.428
	WS0113_N01	04s18240	At2g16850	Plasma membrane intrinsic protein, putative	9e-64	0.687	0.920	1.091	1.501	1.394	1.756	0.647	0.501	0.435
	WS0113_E02	02s17100	At5g08610	DEAD box RNA helicase (RH26)	2e-30	1.448	3.452	1.280	0.834	1.120	1.366	0.414	0.899	0.438
	WS01210_O18	12s12760	At2g40140	Zinc finger (CCCH-type) family protein	4e-07	1.146	1.347	0.972	1.029	1.428	1.318	0.840	1.354	0.438
	WS0232_K18	16s14490	n/a	No significant hit	n/a	0.760	0.497	1.161	1.107	0.858	0.738	0.691	1.454	0.442
	WS0196_L21	06s04820	At2g41710	Ovule development protein, putative	4e-15	0.917	0.624	0.844	1.035	0.777	1.210	0.712	0.692	0.443
	WS01121_M08	09s13470	At2g21050	Amino acid permease, putative	4e-48	0.729	0.856	1.320	1.073	0.888	1.040	0.914	0.698	0.446
	WS0234_G17	12s00760	n/a	No significant hit	n/a	0.809	1.028	1.340	0.874	0.969	1.053	0.868	0.840	0.453
	WS0231_C11	06s03090	At2g41010	65 VQ motif-containing protein	2e-22	0.532	0.430	0.698	0.975	0.943	0.850	0.950	1.089	0.453
	WS0188_G07	12s03800	At1g48430	Dihydroxyacetone kinase family	8e-77	1.090	1.361	1.276	0.805	1.104	0.804	0.773	0.742	0.459
	WS0123_D12	07s03520	At2g22500	Mitochondrial substrate carrier family protein	4e-54	1.397	1.640	1.079	0.647	1.296	1.176	0.931	1.415	0.467

[1]Microarray elements ranked by fold-change (FC) induction of response in SSi leaves to mechanical wounding plus FTC OS vs untreated control at 2 h, 6 h and 24 h, with FC values for those elements from LSo and SSo leaves also included for comparison. Subsequent redundant examples of a gene family at each time point are removed to improve the diversity of different families included. Only FC values with statistical significance ($P < 0.05$, $Q < 0.05$) are coloured as different from '–' ('no change') according to the colour scale shown at right, where dark green to dark red correlates with the listed fold-change in expression. Abbreviations: AGI, *Arabidopsis* genome initiative; *E*-value, Expect-value; OS, oral secretions.
[2]Genome model names have the 'POPTR_00' prefix removed to fit the table.

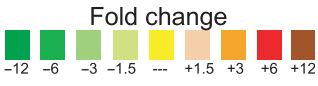

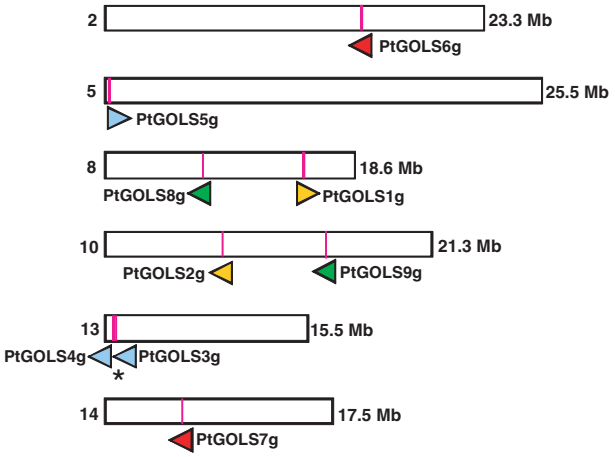

Fig. 5 Genome organization of the *Populus trichocarpa* galactinol synthase (PtGOLS) gene family. The 'g' at end of gene name indicates these are gene models predicted from the most recent assembly of the poplar genome sequence v2.0 (http://www.phytozome.net/poplar). Chromosomes are indicated by their scaffold number to the left of the chromosome representation. Total length of chromosomes is shown to the right in megabases (Mb). Gene orientation is indicated by the arrowhead. Arrowheads of the same colour indicate gene pairs that arose apparently by duplication from a common ancestor. The asterisk indicates tandem duplication.

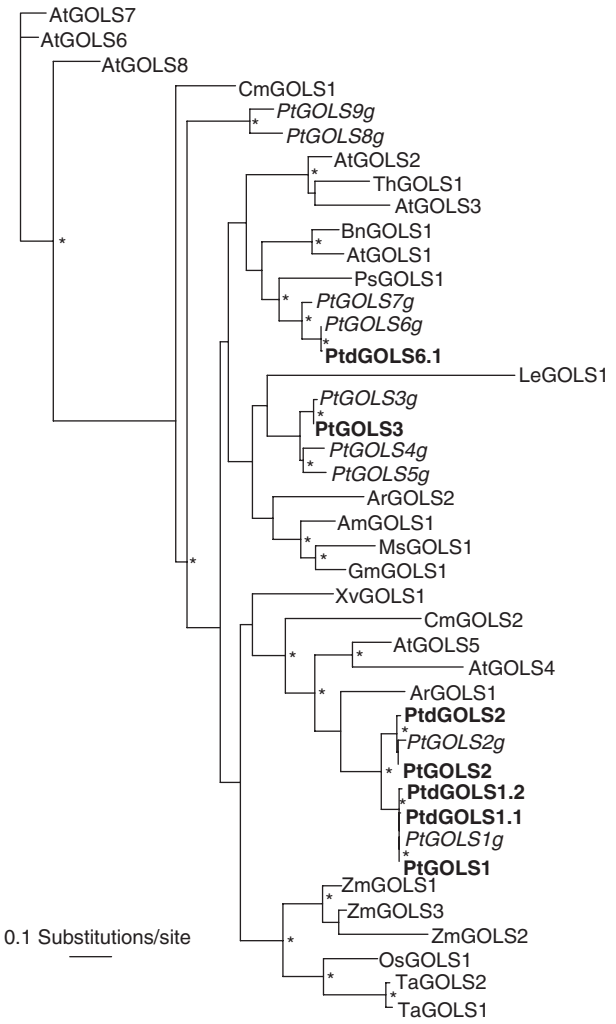

Fig. 6 Phylogeny of the galactinol synthase (GOLS) gene family of poplar and other plant species. Amino acid sequences of 42 proteins were analysed by maximum likelihood using PHYML. Bootstrap values are indicated with an asterisk only for nodes with > 80% support. Genes shown with names in bold represent full-length poplar cDNAs. Genes shown with names in italics and a 'g' are predicted gene models from the *Populus trichocarpa* v2.0 genome sequence assembly (http://www.phytozome.net/poplar). Details for GOLS nomenclature, species names and accession numbers are listed in the Supporting Information, Table S5.

(Sprenger & Keller, 2000) was only partly conserved in poplar GOLSs, with PtGOLS1g possessing an APTAA sequence (on three independent FLcDNA clones) and PtGOLS8g and PtGOLS9g possessing an LPSAA sequence (Fig. S4). A putative manganese-binding motif DXD (Breton *et al.*, 1998; Busch *et al.*, 1998; Wiggins & Munro, 1998) was found in all PtGOLS gene models. A serine phosphorylation site was absent from PtGOLS8g and PtGOLS9g, as is the case with *Arabidopsis thaliana* AtGolS2 and AtGolS3. Phylogenetic comparison of 26 GOLS from other plant species with the nine PtGOLS genes and the seven FLcDNAs showed that the level of sequence divergence among poplar GOLS is similar to the overall divergence across the plant GOLS family (Fig. 6).

GOLS transcripts show source- or sink-specific induction patterns

Expression analysis in source and sink leaves of hybrid poplar in response to OS was done by qPCR to quantify transcripts for four poplar GOLS for which gene-specific primers could be identified and verified by amplicon sequencing (Fig. 7). Before OS treatment GOLS transcripts were present at very low levels in sink leaves, but were expressed at higher levels in source leaves (data not shown). Treatment with OS caused leaf type-specific GOLS induction (Fig. 7). Two GOLS genes, PtdGOLS1.2 and PtdGOLS2.1, which have high constitutive transcript levels in source leaves (not shown) exhibited the greatest increase (*c.* 250-fold) in transcript abundance at 2 h in SSi leaves. By contrast, PtGOLS3.1 expression was upregulated only in SSo leaves but was downregulated in LSo and SSi leaves (*c.* 400-fold up vs 15 000-fold and 10-fold down, respectively). The upregulation of PtGOLS3.1 in SSo was highest at 2 h, whereas the suppression in LSo and SSi was strongest at 24 h. Transcripts of the fourth pGOLS tested (PtdGOLS6.1) were increased *c.* 10-fold in all three leaf types with highest abundance at 2 h in source (LSo and SSo) leaves and at 6 h in distant sink (SSi) leaves.

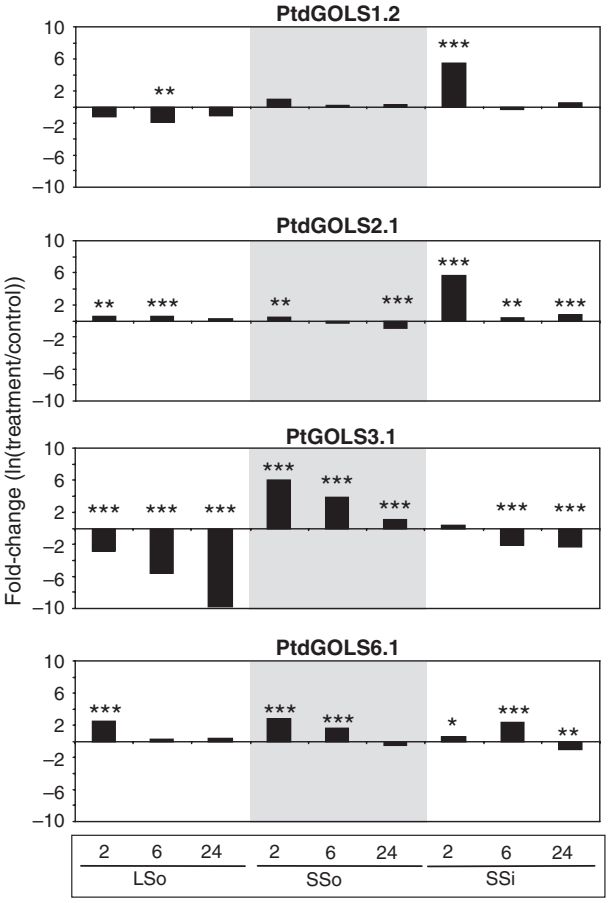

Fig. 7 Quantitative real-time PCR analysis of gene expression of galactinol synthase (GOLS) in poplar leaves in response to simulated forest tent caterpillar (FTC) herbivory. Values represent fold-change differences between leaves from untreated control trees and leaves from trees treated with mechanical wounding plus FTC oral secretion (OS). Transcript abundance was examined in local source (LSo), systemic source (SSo) and systemic sink (SSi) leaves at 2 h, 6 h and 24 h post-treatment. Data were normalized to poplar translation initiation factor 5A (TIF5A; WS0116_J23; POPTR_0006s19870) by subtracting the Ct value of each transcript, where $\Delta Ct = Ct_{transcript} - Ct_{TIF5A}$. Transcript abundance for each gene was obtained from the equation $(1 + E)^{-\Delta Ct}$, where E is the PCR efficiency, as described by Ramakers *et al.* (2003). Fold-change of GOLS transcript abundance was calculated as a treatment/control ratio of relative expression levels. Statistical significance of fold-change differences was determined using a linear model (see the Materials and Methods section and Table S6). Significance thresholds were set at * $P < 0.05$; ** $P < 0.01$; *** $P < 0.001$.

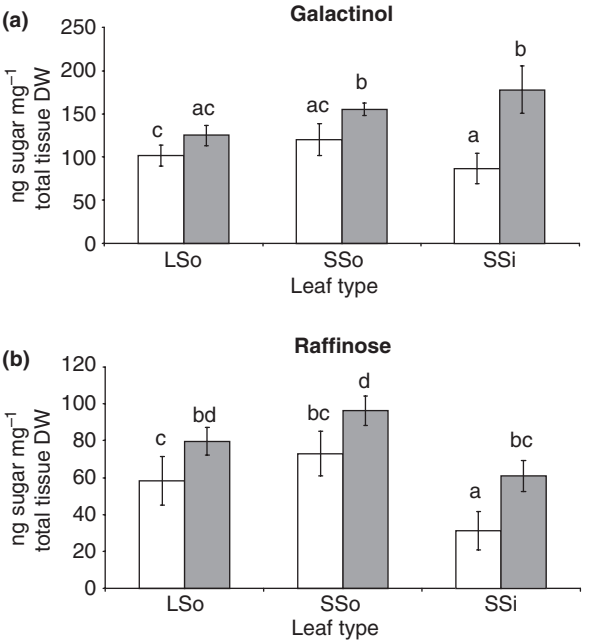

Fig. 8 Changes of levels of galactinol (a) and raffinose (b) in poplar leaves after simulated herbivory. Soluble sugars were isolated from local source (LSo), systemic source (SSo) and systemic sink (SSi) leaves of oral secretion (OS)-treated trees (2 h post-treatment) (tinted bars) and untreated control trees (open bars) and analysed by anion-exchange high pressure liquid chromatography. Values are represented as mean ± SD ($n = 5$ individual trees). Data were analysed separately using two-way ANOVA and Tukey multiple comparison tests. Bars with different letters above them are significantly different at $P = 0.050$; letters are independent such that 'ac' is not significantly different from either 'a' or 'c', while 'a' and 'c' are significantly different from each other.

Rapid increase in galactinol and raffinose in poplar leaves

Next we tested if levels of the sugar alcohol galactinol changed during the OS-induced systemic defense responses in poplar leaves (Fig. 8). Galactinol levels were significantly increased in systemic leaves at 2 h after OS treatment (SSi 2-fold, $P = 0.034$; SSo 1.2-fold, $P = 0.048$). Raffinose, a trisaccharide formed from galactinol and sucrose, also increased significantly in concentration throughout the plant, and again more so in SSi leaves (LSo 1.3-fold, $P = 0.030$; SSo 1.3-fold, $P = 0.016$; SSi 2-fold, $P < 0.001$).

Discussion

Simulated FTC attack

In previous work on the response of poplar to FTC feeding, Major & Constabel (2006) identified FTC OS as a reliable mimic of insect herbivory when OS was added to mechanically wounded leaves. Major & Constabel (2006) identified *N*-hydroxylinolenoyl-L-glutamine, commonly known as volicitin (Alborn *et al.*, 1997), as a potential elicitor in the FTC OS. Because insect feeding involves mechanical damage and contact of wound sites with OS we used a combination of wounding plus OS application to simulate insect attack. Given the complexity of the experimental design of the microarray study with multiple time-points and leaf types, application of OS to wounded leaves served as a practical alternative to actual FTC feeding. Given the large number of samples required for replicated microarray analysis of the

temporal and spatial patterns of the response, we did not attempt to identify the effect of wounding alone. It is therefore important to note that the effects described in this paper are in response to a combined wounding and OS treatment. Furthermore, FTC OS is a complex mixture of compounds (Major & Constabel, 2006). The effect of OS on poplar leaves may depend on variables that were beyond those controlled for in this study. For example, we cannot exclude that the pH of the OS may have had an effect on the response observed in treated leaves. By keeping OS frozen before application we reduced the possible effect of enzymatic degradation of elicitor active compounds in the OS.

Source–sink relationships of systemically responding poplar leaves

Simulated FTC herbivory via mechanical wounding plus FTC OS resulted in a significant increase in CWI activity in both SSo and SSi leaves, similar to the induction of CWI activity in response to jasmonic acid treatment or gypsy moth (*Lymantria dispar*) feeding in *P. trichocarpa* × *nigra* (Arnold & Schultz, 2002). As CWI activity increased in both systemic source and sink leaves, the source–sink relationship was maintained. Insect herbivory has previously been shown to influence carbon partitioning in poplar (Babst *et al.*, 2008).

Transcriptome profiling reveals unique responses in systemic sink tissues

Forest tent caterpillar OS contains active elicitors and can be used as a faithful mimic of insect herbivory in poplar (Major & Constabel, 2006). The OS induces much of the same transcriptome responses as FTC herbivory (Ralph *et al.*, 2006), although the timing of the response varies, with OS treatment causing faster transcriptional responses than FTC feeding, probably owing to a stronger initial stimulus caused by application of OS to a wounded leaf surface compared with the initially small but increasing feeding damage caused by FTC. Previous transcript profiling of poplar responses to wounding or herbivory have identified genes responding locally in treated leaves (Lawrence *et al.*, 2006; Major & Constabel, 2006; Ralph *et al.*, 2006; Babst *et al.*, 2009). Here we went beyond confirming the involvement of many of these previously identified genes in the local defense response of poplar, providing a time-course profile of the transcriptome response in treated leaves. Babst *et al.* (2009) also established transcriptome responses in both local source leaves and in systemic sink leaves in response to herbivory and jasmonic acid (JA) at 22 h after onset of treatment. The later time-points (22 h) of the induced transcriptomes studied by Babst *et al.* (2009) and those identified in this study at 24 h share many similarities. However, the unique earlier response in SSi leaves was not captured in previous work. The results of the present time-course analysis also showed differential timing (i.e. separation in time) of the responses in LSo leaves with early induction of transcripts of oxidative stress response and octadecanoid signalling (e.g. allene oxide cyclase WS0155_D02; POPTR_0004s10240, peaking at 2 h mainly in LSo leaves) and later induction of known or putative defense genes (e.g. Kunitz protease inhibitor WS0151_M13; POPTR_0010s01160, maximum at 24 h in LSo and in SSo and SSi leaves). It remains to be investigated whether the observed changes in gene expression result in altered protein profiles and signalling activities.

In the systemic response, the induced transcriptome change in SSo leaves is weaker and slower than that of LSo leaves; however, a rapid, strong and distinct transcriptome response was activated in distant, juvenile SSi leaves. The early SSi response may allow for increased resource allocation and import into sink leaves for the production of a systemically induced defense at the growing shoot apex. The developing SSi leaves (Fig. 1) may lack constitutive resources to produce these defenses at the levels required (Jones *et al.*, 1993), and resources from source leaves may be necessary to provide substrate for the suite of induced defense genes seen throughout the plant over the 24 h time-course. The strong induction of carbon metabolism genes in the transcriptome response of SSi leaves at 2 h could be a signature of induced increase of carbon resource allocation along source–sink gradients. By contrast, the later transcriptome signatures of sink leaves at 6 h and at 24 h show prominent features of induced defense genes.

GOLS and galactinol in the systemically induced response to biotic stress

The putative role(s) of the raffinose family of oligosaccharides (RFO) in plants include transport and storage of carbon resources and osmoprotectants in response to abiotic stress (Dey, 1985; Bachmann *et al.*, 1994; Haritatos *et al.*, 1996; Sprenger & Keller, 2000; Taji *et al.*, 2002). They are produced by the sequential addition of galactinol units to sucrose. Galactinol is synthesized from UDP-galactose and myo-inositol by GOLS (inositol 3-α-galactosyltransferase; Keller & Pharr, 1996). The addition of one, two or three galactinol units to sucrose yields the trisaccharide raffinose, the tetrasaccharide stachyose, or the pentasaccharide verbascose, respectively (Peterbauer & Richter, 2001). Isoforms of GOLS are differentially expressed during drought, heat, and cold stress in *Arabidopsis thaliana* (Liu *et al.*, 1998; Taji *et al.*, 2002; Cunningham *et al.*, 2003; Panikulangara *et al.*, 2004), and overexpression of GOLS in *A. thaliana* leads to enhanced drought tolerance (Taji *et al.*, 2002). Here we showed differential induction of some of the poplar GOLS genes with gene-specific patterns in source and sink leaves in response to simulated herbivore feeding. The involvement of GOLS in both abiotic and biotic stress responses

perhaps points to a general role for GOLS and galactinol in stress-induced changes of carbon metabolism and reallocation of carbon resources. Indeed, while salt stress strongly induces GOLS isoforms in *Populus euphratica*, the galactinol produced does not itself play a direct role as compatible solute in osmoregulation in this species (Ottow *et al.*, 2005). It is also possible that galactinol could be a component of systemic defense signalling.

Possible signals involved in activation of systemic defense response in poplar

Simulated FTC herbivory elicited a cascade of transcriptome responses in local and systemic and in source and sink leaves. The responses of the different leaf types vary in the genes involved, as well as in their temporal patterns of expression and overall magnitude of change. Transcripts from different signalling pathways changed in abundance throughout the plant, though some were leaf-type specific. For example, genes involved in JA signalling were upregulated throughout the plant, but more strongly and rapidly in LSo than in SSo and SSi leaves. Similarly, genes involved in ethylene signalling were upregulated most strongly in LSo leaves. On the other hand 9-*cis*-epoxycarotenoid dioxygenase, involved in ABA synthesis, was strongly and transiently upregulated in SSi leaves at the 2 h timepoint (Fig. 3; Table S3). A possible role for ABA in the defense response of SSi leaves would be supported by the upregulation of ABA-sensing proteins in sink leaves in response to herbivory (Babst *et al.*, 2009). Several genes for calcium signalling responded strongly at 2 h in SSi leaves, supporting findings of OS-induced calcium signalling in the early response to insect herbivory (Maffei *et al.*, 2004; Lippert *et al.*, 2009). Given the changes in soluble sugars, it is also noteworthy that transcription of a number of genes responding in SSi leaves is known or proposed to be controlled by soluble sugars (Rolland *et al.*, 2002).

The rapid response in SSi leaves requires a signal that moves at a rate similar to that measured for phloem transport (50–100 cm h^{-1}; Canny, 1975) in order to elicit transcriptional changes of the magnitude observed by 2 h in SSi leaves that are *c.* 150 cm away in an acropetal direction from the LSo leaves. Such a signal could involve jasmonates (Li *et al.*, 2002; Howe, 2004), sugar sensing (Ehness *et al.*, 1997; Rolland *et al.*, 2002) or other signals (Lautner *et al.*, 2005; Frost *et al.*, 2007; Maffei *et al.*, 2007; Pandey *et al.*, 2008). The nature of the systemic signal(s) in poplar remains to be identified in future work. It is possible that the dynamic pattern of transcriptome responses observed in SSi leaves at 2 h, 6 h and 24 h results from a combination of signals acting in sequential cascades to produce an early reallocation of resource and culminating in the systemically induced response of defense genes.

Conclusions

Distinct spatial and temporal transcriptome patterns are induced by simulated insect attack in local and systemic, source and sink leaves of poplar. Induced transcriptome cascades are associated with induction of cell wall invertase activity, enhancement of source–sink relationships, leaf type specific changes of galactinol synthase gene expression and concomitant increase in galactinol and raffinose levels. Systemic transcriptome changes of SSi leaves are rapid and strong with initial signatures of metabolism and signalling, followed by induction of defense genes.

Acknowledgements

We thank Rick White for help with experimental design and statistical analysis, Sharon Janscik for help with cDNA preparation, David Kaplan for greenhouse support, Sarah Martz for OS collection, Elizabeth Chun and Mack Yuen for bioinformatics assistance, and Bob McCron for supply of FTC. This work was supported by the Natural Science and Engineering Research Council of Canada (NSERC) (grant to J.B., fellowship to R.N.P.), Genome British Columbia, and Genome Canada (grant to J.B.). Salary support for J.B. was provided in part by the University of British Columbia Distinguished Scholar Program.

References

Alborn T, Turlings TCJ, Jones TH, Stenhagen G, Loughrin JH, Tumlinson JH. 1997. An elicitor of plant volatiles from beet armyworm oral secretion. *Science* **276**: 945–949.

Arimura G-I, Huber DPW, Bohlmann J. 2004. Forest tent caterpillars (*Malacosoma disstria*) induce local and systemic diurnal emissions of terpenoid volatiles in hybrid poplar (*Populus trichocarpa* × *deltoides*): cDNA cloning, functional characterization, and patterns of gene expression of (−)-germacrene D synthase, PtdTPS1. *Plant Journal* **37**: 603–616.

Arnold T, Appel H, Patel V, Stocum E, Kavalier A, Schultz J. 2004. Carbohydrate translocation determines the phenolic content of *Populus* foliage: a test of the sink–source model of plant defense. *New Phytologist* **164**: 157–164.

Arnold TM, Schultz JC. 2002. Induced sink strength as a prerequisite for induced tannin biosynthesis in developing leaves of *Populus*. *Oecologia* **130**: 585–593.

Babst BA, Ferrieri RA, Thorpe MR, Orians CM. 2008. *Lymantria dispar* herbivory induces rapid changes in carbon transport and partitioning in *Populus nigra*. *Entomologia Experimentalis et Applicata* **128**: 117–125.

Babst BA, Sjodin A, Jansson S, Orians C. 2009. Local and systemic transcriptome responses to herbivory and jasmonic acid in *Populus*. *Tree Genetics and Genomes* **5**: 459–474.

Bachmann M, Matile P, Keller F. 1994. Metabolism of the raffinose family oligosaccharides in leaves of *Ajuga reptans* – cold-acclimation, translocation, and sink to source transition – discovery of chain elongation enzyme. *Plant Physiology* **105**: 1335–1345.

Baldwin IT. 1998. Jasmonate-induced responses are costly but benefit plants under attack in native populations. *Proceedings of the National Academy of Sciences, USA* **95**: 8113–8118.

Brazma A, Hingamp P, Quackenbush J, Sherlock G, Spellman P, Stoeckert C, Aach J, Ansorge W, Ball CA, Causton HC *et al.* 2001. Minimum information about a microarray experiment (MIAME) – toward standards for microarray data. *Nature Genetics* **29**: 365–371.

Breton C, Bettler E, Joziasse DH, Geremia RA, Imberty A. 1998. Sequence–function relationships of prokaryotic and eukaryotic galactosyltransferases. *Journal of Biochemistry* **123**: 1000–1009.

Bryan J. 2004. Problems in gene clustering based on gene expression data. *Journal of Multivariate Analysis* **90**: 44–66.

Busch C, Hofmann F, Selzer J, Munro S, Jeckel D, Aktories K. 1998. A common motif of eukaryotic glycosyltransferases is essential for the enzyme activity of large clostridial cytotoxins. *Journal of Biological Chemistry* **273**: 19566–19572.

Canny MJP. 1975. Mass transfer. In: Zimmermann HM, Milburn JA, eds. *Encylopedia of plant physiology*. Berlin, Germany: Springer, 139–153.

Christopher ME, Miranda M, Major IT, Constabel CP. 2004. Gene expression profiling of systemically wound-induced defenses in hybrid poplar. *Planta* **219**: 936–947.

Cunningham SM, Nadeau P, Castonguay Y, Laberge S, Volenec JJ. 2003. Raffinose and stachyose accumulation, galactinol synthase expression, and winter injury of contrasting alfalfa germplasms. *Crop Science* **43**: 562–570.

Davis JM, Gordon MP, Smit BA. 1991. Assimilate movement dictates remote sites of wound-induced gene-expression in poplar leaves. *Proceedings of the National Academy of Sciences, USA* **88**: 2393–2396.

Dey PM. 1985. *D*-galactose-containing oligosaccharides. In: Dey PM, Dixon RA, eds. *Biochemistry of storage carbohydrates in green plant*. London, UK: Academic Press, 53–129.

Ehness R, Ecker M, Godt DE, Roitsch T. 1997. Glucose and stress independently regulate source and sink metabolism and defense mechanisms via signal transduction pathways involving protein phosphorylation. *Plant Cell* **9**: 1825–1841.

Felsenstein J. 1993. *PHYLIP (Phylogeny Inference Package) Version 3.5c*. (evolution.genetics.washington.edu/phylip.html)

Frost CJ, Appel HM, Carlson JE, De Moraes CM, Mescher MC, Schultz JC. 2007. Within-plant signalling via volatiles overcomes vascular constraints on systemic signalling and primes responses against herbivores. *Ecology Letters* **10**: 490–498.

Gascuel O. 1997. BioNJ: an improved version of the NJ algorithm based on a simple model of sequence data. *Molecular Biology and Evolution* **14**: 685–695.

Guindon S, Gascuel O. 2003. A simple, fast, and accurate algorithm to estimate large phylogenies by maximum likelihood. *Systematic Biology* **52**: 696–704.

Haritatos E, Keller F, Turgeon R. 1996. Raffinose oligosaccharide concentrations measured in individual cell and tissue types in *Cucumis melo* leaves: implications for phloem loading. *Planta* **198**: 614–622.

Havill NP, Raffa KF. 1999. Effects of elicitation treatment and genotypic variation on induced resistance in *Populus*: impacts on gypsy moth (Lepidoptera : Lymantriidae) development and feeding behavior. *Oecologia* **120**: 295–303.

Howe GA. 2004. Jasmonates as signals in the wound response. *Journal of Plant Growth Regulation* **23**: 223–237.

Huang XQ, Madan A. 1999. CAP3: a DNA sequence assembly program. *Genome Research* **9**: 868–877.

Jones CG, Hopper RF, Coleman JS, Krischik VA. 1993. Control of systemically induced herbivore resistance by plant vascular architecture. *Oecologia* **93**: 452–456.

Jones DT, Taylor WR, Thornton JM. 1992. The rapid enumeration of mutation data matrices from protein sequences. *Computer Applications in the Biosciences* **8**: 275–282.

Keller F, Pharr DM. 1996. Metabolism of carbohydrates in sinks and sources: galactosyl-sucrose oligosaccharides. In: Zamski E, Schaffer AA, eds. *Photoassmilate distribution in plants and crop*. New York, NY, USA: Marcel Dekker, 115–184.

Kolosova N, Miller B, Ralph S, Ellis BE, Douglas C, Ritland K, Bohlmann J. 2004. Isolation of high-quality RNA from gymnosperm and angiosperm trees. *BioTechniques* **36**: 821–824.

Larson PR. 1979. Establishment of the vascular system in seedlings of *Populus deltoides* Bartr. *American Journal of Botany* **66**: 452–462.

Larson PR, Isebrands JG. 1971. The plastochron index as applied to developmental studies of cottonwood. *Canadian Journal of Forest Research* **1**: 1–11.

Lautner S, Grams TEE, Matyssek R, Fromm J. 2005. Characteristics of electrical signals in poplar and responses in photosynthesis. *Plant Physiology* **138**: 2200–2209.

Lawrence SD, Dervinis C, Novak N, Davis JM. 2006. Wound and insect herbivory responsive genes in poplar. *Biotechnology Letters* **28**: 1493–1501.

Li L, Chuanyou L, Lee GI, Howe GA. 2002. Distinct roles for jasmonate synthesis and action in the systemic wound response of tomato. *Proceedings of the National Academy of Sciences, USA* **99**: 6416–6421.

Lippert DN, Ralph SG, Phillips M, White R, Smith D, Hardie D, Gershenzon J, Ritland K, Borchers CH, Bohlmann J. 2009. Quantitative iTRAQ proteome and comparative transcriptome analysis of elicitor-induced Norway spruce (*Picea abies*) cells reveals elements of calcium signaling in the early conifer defense response. *Proteomics* **9**: 350–367.

Liu JJJ, Krenz DC, Galvez AF, de Lumen BO. 1998. Galactinol synthase (GS): increased enzyme activity and levels of mRNA due to cold and desiccation. *Plant Science* **134**: 11–20.

Maffei M, Bossi S, Spiteller D, Mithofer A, Boland W. 2004. Effects of feeding *Spodoptera littoralis* on lima bean leaves. I. Membrane potentials, intracellular calcium variations, oral secretions, and regurgitate components. *Plant Physiology* **134**: 1752–1762.

Maffei ME, Mithofer A, Boland W. 2007. Before gene expression: early events in plant-insect interaction. *Trends in Plant Science* **12**: 310–316.

Major IT, Constabel CP. 2006. Molecular analysis of poplar defense against herbivory: comparison of wound- and insect elicitor-induced gene expression. *New Phytologist* **172**: 617–635.

Mauricio R. 1998. Costs of resistance to natural enemies in field populations of the annual plant *Arabidopsis thaliana*. *American Naturalist* **151**: 20–28.

Miller LG. 1959. Use of dinitrosalicylic acid reagent for determination of reducing sugar. *Analytical Chemistry* **31**: 426–428.

Miranda M, Ralph SG, Mellway R, White R, Heath MC, Bohlmann J, Constabel CP. 2007. The transcriptional response of hybrid poplar (*Populus trichocarpa* × *deltoides*) to infection by *Melampsora medusae* leaf rust involves induction of flavonoid pathway genes leading to the accumulation of proanthocyanidins. *Molecular Plant–Microbe Interactions* **20**: 816–831.

Ottow EA, Brinker M, Teichmann T, Fritz E, Kaiser W, Brosche M, Kangasjarvi J, Jiang XN, Polle A. 2005. *Populus euphratica* displays apoplastic sodium accumulation, osmotic adjustment by decreases in calcium and soluble carbohydrates, and develops leaf succulence under salt stress. *Plant Physiology* **139**: 1762–1772.

Page RDM. 1996. Treeview: an application to display phylogenetics trees on personal computers. *Computer Applications in the Biosciences* **12**: 357–358.

Pandey SP, Shahi P, Gase K, Baldwin IT. 2008. Herbivory-induced changes in the small-RNA transcriptome and phytohormone signaling in *Nicotiana attenuata*. *Proceedings of \the National Academy of Sciences, USA* **105**: 4559–4564.

Panikulangara TJ, Eggers-Schumacher G, Wunderlich M, Stransky H, Schoffl F. 2004. *Galactinol synthase1*. A novel heat shock factor target

gene responsible for heat-induced synthesis of raffinose family oligosaccharides in *Arabidopsis*. *Plant Physiology* **136**: 3148–3158.

Parsons TJ, Bradshaw HD, Gordon MP. 1989. Systemic accumulation of specific mRNAs in response to wounding in poplar trees. *Proceedings of the National Academy of Sciences, USA* **86**: 7895–7899.

Peterbauer T, Richter A. 2001. Biochemistry and physiology of raffinose family oligosaccharides and galactosyl cyclitols in seeds. *Seed Science Research* **11**: 185–197.

Philippe RN, Bohlmann J. 2007. Poplar defense against insect herbivores. *Canadian Journal of Botany-Revue Canadienne De Botanique* **85**: 1111–1126.

Philippe RN, Ralph SG, Kulheim C, Jancsik SI, Bohlmann J. 2009. Poplar defense against insects: genome analysis, full-length cDNA cloning, and transcriptome and protein analysis of the poplar Kunitz-type protease inhibitor family. *New Phytologist* **184**: 865–884.

Ralph SG. 2009. Studying *Populus* defenses against insect herbivores in the post-genomic era. *Critical Reviews in Plant Sciences* **28**: 335–345.

Ralph SG, Chun HJE, Cooper D, Kirkpatrick R, Kolosova N, Gunter L, Tuskan GA, Douglas CJ, Holt RA, Jones SJM *et al.* 2008. Analysis of 4,664 high-quality sequence-finished poplar full-length cDNA clones and their utility for the discovery of genes responding to insect feeding. *BMC Genomics* **9**. Article #57.

Ralph S, Oddy C, Cooper D, Yueh H, Jancsik S, Kolosova N, Philippe RN, Aeschliman D, White R, Huber D *et al.* 2006. Genomics of hybrid poplar (*Populus trichocarpa* × *deltoides*) interacting with forest tent caterpillars (*Malacosoma disstria*): normalized and full-length cDNA libraries, expressed sequence tags, and a cDNA microarray for the study of insect-induced defences in poplar. *Molecular Ecology* **15**: 1275–1297.

Ramakers C, Ruijter JM, Deprez RHL, Moorman AFM. 2003. Assumption-free analysis of quantitative real-time polymerase chain reaction (PCR) data. *Neuroscience Letters* **339**: 62–66.

Rolland F, Moore B, Sheen J. 2002. Sugar sensing and signalling in plants. *Plant Cell* **14**: S185–S205.

Sprenger N, Keller F. 2000. Allocation of raffinose family oligosaccharides to transport and storage pools in *Ajuga reptans*: the roles of two distinct galactinol synthases. *Plant Journal* **21**: 249–258.

Strauss SY, Rudgers JA, Lau JA, Irwin RE. 2002. Direct and ecological costs of resistance to herbivory. *Trends in Ecology and Evolution* **17**: 278–285.

Taji T, Ohsumi C, Iuchi S, Seki M, Kasuga M, Kobayashi M, Yamaguchi-Shinozaki K, Shinozaki K. 2002. Important roles of drought- and cold-inducible genes for galactinol synthase in stress tolerance in *Arabidopsis thaliana*. *Plant Journal* **29**: 417–426.

Tuskan GA, DiFazio S, Jansson S, Bohlmann J, Grigoriev I, Hellsten U, Putnam N, Ralph S, Rombauts S, Salamov A *et al.* 2006. The genome of black cottonwood, *Populus trichocarpa* (Torr. & Gray). *Science* **313**: 1596–1604.

Whitham TG, Floate KD, Martinsen GD, Driebe EM, Keim P. 1996. Ecological and evolutionary implications of hybridization: *Populus*–herbivore interactions. In: Stettler RF, Bradshaw HD, Heilman PE, Hinckley TM, eds. *Biology of* Populus *and its implications for management and conservation*. Ottawa, ON, Canada: NRC Research Press, 247–275.

Wiggins CAR, Munro S. 1998. Activity of the yeast MNN1 alpha-1,3-mannosyltransferase requires a motif conserved in many other families of glycosyltransferases. *Proceedings of the National Academy of Sciences, USA* **95**: 7945–7950.

Supporting Information

Additional supporting information may be found in the online version of this article.

Fig. S1 Schematic of microarray hybridization design.

Fig. S2 Comparison of variance and response obtained by microarray hybridizations using samples from individual trees separately or as pooled samples.

Fig. S3 Overall spatial and temporal patterns of differentially expressed (DE) genes in local and systemic leaves in response to forest tent caterpillar (FTC) oral secretions (OS) detected by transcriptome analysis on a microarray platform of 15 496 cDNA elements.

Fig. S4 Amino acid sequence alignment of galactinol synthases.

Table S1 Complete set of systemic microarray experiment results

Table S2 Oligonucleotide primers used in quantitative real-time PCR analyses

Table S3 Quantitative real-time PCR analysis for validation of microarray results

Table S4 Clustering analysis of microarray results

Table S5 Amino acid sequence relatedness of plant galactinol synthases

Table S6 Quantitative real-time PCR analysis of poplar galactinol synthase systemic expression

Methods S1 Microarray analysis and quantitative real-time PCR validation.

Please note: Wiley-Blackwell are not responsible for the content or functionality of any supporting information supplied by the authors. Any queries (other than missing material) should be directed to the *New Phytologist* Central Office.